

# Geochemical assessment of the palaeoecology, ontogeny, morphotypic variability and palaeoceanographic utility of "Dentoglobigerina" venezuelana

Stewart, Joseph A.; Wilson, Paul A.; Edgar, Kirsty M.; Anand, Pallavi; James, Rachael H.

DOI:  
[10.1016/j.marmicro.2011.11.003](https://doi.org/10.1016/j.marmicro.2011.11.003)

License:  
Creative Commons: Attribution-NonCommercial-NoDerivs (CC BY-NC-ND)

*Document Version*  
Peer reviewed version

*Citation for published version (Harvard):*  
Stewart, JA, Wilson, PA, Edgar, KM, Anand, P & James, RH 2012, 'Geochemical assessment of the palaeoecology, ontogeny, morphotypic variability and palaeoceanographic utility of "Dentoglobigerina" venezuelana', *Marine Micropalaeontology*, vol. 84-85, pp. 74-86. <https://doi.org/10.1016/j.marmicro.2011.11.003>

[Link to publication on Research at Birmingham portal](#)

**Publisher Rights Statement:**  
Published in *Marine Micropaleontology* on 25/11/2011

DOI: 10.1016/j.marmicro.2011.11.003

## General rights

Unless a licence is specified above, all rights (including copyright and moral rights) in this document are retained by the authors and/or the copyright holders. The express permission of the copyright holder must be obtained for any use of this material other than for purposes permitted by law.

- Users may freely distribute the URL that is used to identify this publication.
- Users may download and/or print one copy of the publication from the University of Birmingham research portal for the purpose of private study or non-commercial research.
- User may use extracts from the document in line with the concept of 'fair dealing' under the Copyright, Designs and Patents Act 1988 (?)
- Users may not further distribute the material nor use it for the purposes of commercial gain.

Where a licence is displayed above, please note the terms and conditions of the licence govern your use of this document.

When citing, please reference the published version.

## Take down policy

While the University of Birmingham exercises care and attention in making items available there are rare occasions when an item has been uploaded in error or has been deemed to be commercially or otherwise sensitive.

If you believe that this is the case for this document, please contact [UBIRA@lists.bham.ac.uk](mailto:UBIRA@lists.bham.ac.uk) providing details and we will remove access to the work immediately and investigate.

1 **Geochemical assessment of the palaeoecology, ontogeny,**  
 2 **morphotypic variability and palaeoceanographic utility of**  
 3 ***“Dentoglobigerina” venezuelana***

4 **Joseph A. Stewart <sup>a,\*</sup>, Paul A. Wilson <sup>a</sup>, Kirsty M. Edgar <sup>a,†</sup>, Pallavi Anand <sup>b</sup>, Rachael H. James <sup>a</sup>**

5 <sup>a</sup>National Oceanography Centre, Southampton, University of Southampton. SO14 3ZH, UK.

6 <sup>†</sup>Now at: School of Earth and Ocean Sciences, Cardiff University, Main Building, Park Place, Cardiff, CF10 3AT, UK

7 <sup>b</sup>Department of Earth and Environmental Science, Walton Hall, The Open University, Milton Keynes, MK7 6AA, UK

8 \*Corresponding author. Tel: +442380599374, Email: Joseph.Stewart@noc.soton.ac.uk

9 **1. Introduction**

10 There is a pressing need to improve our understanding of Oligo-Miocene (O/M) climate  
 11 change and, in particular, the major perturbation of Cenozoic climate that occurred near the  
 12 O/M boundary at around 23 Ma (Figure 1). This climate shift is marked by a large increase  
 13 in the benthic foraminifera  $\delta^{18}\text{O}$  record ( $>1.5\%$ ), classically termed the “Mi-1 event” (after  
 14 the “Mi-1 zone” of Miller et al., 1991), that is now well dated cyclo- and  
 15 magnetostratigraphically to “58<sub>Ol-C6cn</sub>” in the scheme of Wade and Pälike, (2004) and Pälike  
 16 et al., (2006b). The increase in benthic  $\delta^{18}\text{O}$  is interpreted to represent major ice sheet  
 17 expansion on Antarctica (Zachos et al., 2001) associated with a contemporaneous change in  
 18 the carbon cycle as indicated by an increase in  $\delta^{13}\text{C}$  of benthic foraminifera (Figure 1).

19 While benthic foraminiferal  $\delta^{18}\text{O}$  records provide insight into the timing and magnitude of  
 20 glaciation, the causes and consequences of the Mi-1 event remain poorly understood. An  
 21 increase in the ratio of organic carbon to carbonate burial has been invoked (Paul et al., 2000)  
 22 to account for the  $\delta^{13}\text{C}$  maximum shown in Figure 1, however, there is little evidence of  
 23 organic carbon-rich deposits of appropriate age (Lear et al., 2004). Changes in global silicate  
 24 weathering have a profound effect on the global carbon cycle and climate change on multi-  
 25 million year timescales (Berner, 1991; Raymo and Ruddiman, 1992; Walker et al., 1981), but  
 26 relatively little is known about the links between short-term ( $<10^5$  yrs) climatic aberrations  
 27 and silicate weathering (Vance et al., 2009). Nevertheless, variations in chemical weathering  
 28 rates (and therefore levels of atmospheric carbon dioxide), related to the degree of silicate  
 29 rock exposure on Antarctica, are hypothesised to account for temperature anomalies observed  
 30 across the O/M boundary (Lear et al., 2004; cf. Kump et al., 1999). A detailed assessment of  
 31 silicate weathering across the O/M interval is therefore needed to help assess linkages  
 32 between climate change and this major geological sink for atmospheric  $\text{CO}_2$ .

33 Silicate weathering is known to exert a control on the oceanic concentration and isotopic  
 34 composition of many elements including Li, Os and Nd (Burton and Vance, 2000; Frank,  
 35 2002; Huh et al., 2001; Kiskurek et al., 2005; Ravizza and Peucker-Ehrenbrink, 2003).

36 Arguably the most useful archive for reconstructing the palaeoceanographic record of silicate  
37 weathering through use of these elements is planktic foraminiferal calcite recovered from  
38 deep-sea sediment cores as exemplified by the pioneering work of Hathorne and James,  
39 (2006), Vance and Burton, (1999) and Burton et al., (2010). Unfortunately, all of these  
40 elements occur in extremely low abundance within foraminiferal calcite, hence the mass of  
41 carbonate required for isotopic analysis is so large (e.g., Nd ~30 mg; Vance and Burton,  
42 1999) that these proxies cannot readily be applied using typical sample suites. One strategy to  
43 circumvent this problem is to target particularly large, abundant, long-ranging and  
44 cosmopolitan taxa. Such species are rare, but one clear candidate is "*D.*" *venezuelana*, a  
45 species that ranges from the early Oligocene to early Pliocene (Bolli and Saunders, 1989;  
46 Kennett and Srinivasan, 1983; Olsson et al., 2006; Stainforth et al., 1975), typically possesses  
47 medium to large tests (usually 355-400  $\mu\text{m}$ ; Spezzaferri, 1994), has a wide geographical  
48 distribution (equator to  $\sim 50^\circ$  latitude; Spezzaferri, 1994) and is found in high abundance in  
49 tropical O/M sections (Chaisson and Leckie, 1993; Leckie et al., 1993; Pearson and Chaisson,  
50 1997; Spezzaferri, 1994). Yet considerable taxonomic and ecological uncertainties are  
51 associated with "*D.*" *venezuelana* and these must be addressed before this taxon can be used  
52 for palaeoceanographic purposes with any degree of confidence.

53 The brief taxonomic description of the holotype specimen (Hedberg, 1937) has led to  
54 inclusion of multiple morphotypes under "*D.*" *venezuelana* (Kennett and Srinivasan, 1983;  
55 Li et al., 2002; Spezzaferri, 1994; Stainforth et al., 1975), the geochemical validity of which  
56 has never been systematically explored. In addition, the depth ecology of "*D.*" *venezuelana*  
57 is extremely unclear (Figure 2). Most stable isotope studies of planktic foraminifera assign  
58 "*D.*" *venezuelana* to a sub-thermocline habitat (Barrera et al., 1985; Hodell and  
59 Vayavananda, 1993; Keller, 1985; Norris et al., 1993; Pearson et al., 2001; Pearson and  
60 Shackleton, 1995; Smart and Thomas, 2006; Spezzaferri and Pearson, 2009). However, data  
61 generated on samples of O/M boundary age ( $\sim 23$  Ma), from Ceara Rise and Trinidad, imply  
62 that "*D.*" *venezuelana* calcified higher in the water column, within the thermocline (Biolzi,  
63 1983; Pearson et al., 1997; Pearson and Wade, 2009). Furthermore, results from analysis of  
64 Oligocene ( $\sim 28$  Ma) age samples from the Gulf of Mexico (Poore and Matthews, 1984) and  
65 the equatorial Pacific at ODP Site 1218 (Wade et al., 2007), imply that calcification took  
66 place within the mixed layer. Establishing the depth habitat of calcification for "*D.*"  
67 *venezuelana* across the O/M boundary is a prerequisite for the generation of proxy records of  
68 silicate weathering because the concentration of neodymium, and its isotopic composition,  
69 vary with depth in the water column (Jeandel, 1993). Similarly, the Li/Ca of planktic

70 foraminifera may be partly dependent on parameters that change with depth in seawater, such  
71 as carbonate ion saturation state (Hall and Chan, 2004).

72 Here, we present new  $\delta^{18}\text{O}$ ,  $\delta^{13}\text{C}$  and Mg/Ca data from planktic foraminiferal assemblages at  
73 ODP Site 925 (Ceara Rise, equatorial Atlantic Ocean) (Figure 2) of O/M boundary age. We  
74 determine the effect of test size on  $\delta^{18}\text{O}$ ,  $\delta^{13}\text{C}$  and Mg/Ca, and use these data to explore the  
75 ontogenetic variation in the depth habitat of “*D.*” *venezuelana*. We apply a narrow  
76 taxonomic concept to “*D.*” *venezuelana*, by identifying three distinct morphotypes. The  
77 depth habitat of these morphotypes is inferred from  $\delta^{18}\text{O}$  and  $\delta^{13}\text{C}$  analyses, and the  
78 geochemical variation within and between morphotypes is established to assess the validity  
79 of pooling these intra-specific groups for the purpose of generating “sample hungry”  
80 palaeoceanographic records of silicate weathering (e.g., Nd & Li isotopes).

## 81 **2. Materials and Methods**

### 82 **2.1. Geological setting & chronology**

83 Four samples (see Table 1), spanning the O/M boundary, were analysed from core sediments  
84 recovered from ODP Leg 154, Site 925, Hole A (4°12.249'N, 43°29.334'W, 3042.2 m present  
85 water depth; Shipboard Scientific Party, 1995a). Magnetostratigraphic age control is not  
86 available in ODP Leg 154 sediments, but a high quality magnetostratigraphy is available for  
87 ODP Site 1090, Agulhas Ridge (Billups et al., 2002; Channell et al., 2003) and it is correlated  
88 to ODP Site 926 (Liebrand et al., 2011), a close neighbour to our study site (ODP Site 925).  
89 We tie the ODP Site 925 depth scale to that of ODP Site 926 by peak-matching shipboard  
90 magnetic susceptibility and colour reflectance data from both sites. Depth correlation is aided  
91 by astronomically matched tie points on either side of the O/M boundary (work of Crowhurst  
92 and Shackleton; S. Crowhurst personal written communication<sup>1</sup>, 2010) and two  
93 biostratigraphic tie points, the first occurrence of *Paragloborotalia kugleri* and the last  
94 occurrence of *Sphenolithus delphix* (Pearson and Chaisson, 1997; Shipboard Scientific Party,  
95 1995a; Shipboard Scientific Party, 1995b; Weedon et al., 1997). Sample ages are reported  
96 relative to the astronomically tuned age model of ODP Site 926 (Pälike et al., 2006a).

### 97 **2.2. Taxonomy & morphotypes**

98 In some taxonomic descriptions, the final chamber of “*D.*” *venezuelana* is described as flat,  
99 and often small and irregular relative to the penultimate chamber (Spezzaferri, 1994;  
100 Stainforth et al., 1975), whereas in other cases chambers in the final whorl are described as  
101 increasing regularly in size including specimens with a more inflated final chamber and  
102 lobulate test outline (Kennett and Srinivasan, 1983; Li et al., 2002). “*D.*” *venezuelana* has a

103 relatively narrow umbilical aperture compared to other *Dentoglobigerina* species such as *D.*  
104 *altispira* and *D. globosa*, however, discrepancies also exist in the description of this primary  
105 aperture. One study describes the aperture as broadly rectangular or “letter-box” in shape  
106 (Kennett and Srinivasan, 1983). A more recent description by Spezzaferri (1994), however,  
107 suggests a low-arched aperture in “*D.*” *venezuelana*. Disparity among descriptions of the  
108 aperture style likely stem from the low arched aperture seen in the holotype specimen  
109 (Hedberg, 1937) and its non-inclusion in the holotype description. The presence of rare  
110 supplementary apertures is noted in the holotype description (Hedberg, 1937), however, we  
111 find no examples of this species possessing supplementary apertures within our samples.  
112 Umbilical teeth are present on the (pen)ultimate chamber(s) of this taxon (see Plate 1), but  
113 are variable in size, and can be broken and/or obscured by sediment infilling of the aperture.  
114 Hence we do not recommend over-reliance on the presence or absence of umbilical teeth as a  
115 defining morphological characteristic when picking specimens for generating  
116 palaeoceanographic records.

117 To help shed light on these taxonomic issues and to assess the geochemical relevance of the  
118 variable morphological concepts, we separate “*D.*” *venezuelana* into three distinct  
119 morphotypes: 1, specimens with a kummerform, flattened, final chamber and rectangular  
120 aperture (Plate 1.1a-f); 2, individuals possessing kummerform, flattened, final chambers and  
121 low arched (often asymmetrical) apertures (Plate 1.2a-f); and 3, specimens with a large,  
122 embracing final chamber and rectangular aperture (Plate 1.3a-f). In some specimens of  
123 morphotype 2 it is difficult to distinguish the cantilevered final chamber from a bulla (for  
124 example Plate 1.2a). Every effort is made to verify that these are true final chambers through  
125 high magnification examination of the aperture and chamber arrangement in all views,  
126 however, in the absence of a final chamber tooth (for example Plate 1.2d), it is almost  
127 impossible to definitively show this is not a bulla. All morphotypes have tests with a broadly  
128 circular profile, low trochospire and four ovate chambers in the final whorl. All specimens  
129 possess the coarse cancellate wall texture characteristic of “*D.*” *venezuelana*.

### 130 **2.3. Sample preparation**

131 Samples were dried in an oven at 50°C, then gently disaggregated in deionised water using a  
132 shaker table and washed over a 63 µm sieve. Single species of foraminifera were then picked  
133 from multiple size fractions (212-250, 250-300, 300-355, 355-400, 400-450, 450-500 µm) to  
134 obtain 1.2 mg of test calcite per size fraction for each species. Specifically, the three  
135 morphotypes of “*D.*” *venezuelana* were picked along with *Catapsydrax ciproensis*,  
136 *Catapsydrax dissimilis*, *Catapsydrax indianus*, *Globigerinoides altiapertura*, *Globigerina*

137 *bulloides*, “*Globigerinoides*” *primordius*, *Paragloborotalia bella*, and *Paragloborotalia*  
138 *siakensis/mayeri* (Plate 2). Two species of benthic foraminifera, *Cibicidoides mundulus* and  
139 *Oridorsalis umbonatus* were also picked for comparison with planktic foraminifera. All tests  
140 within each species, single size fraction separate were gently broken open between two glass  
141 slides under the light microscope, homogenised and then split. Approximately 200 µg of each  
142 sample was used for stable isotope analysis. Where enough material was available, 1 mg of  
143 mono-specific broken-open test calcite was analysed for Mg/Ca.

#### 144 **2.4. Stable isotope analysis**

145 Samples were ultrasonicated in deionised water to remove clays and other adhering particles  
146 before analysis of stable carbon and oxygen isotopes by a gas source mass spectrometer  
147 (Europa GEO 20-20) equipped with an automatic carbonate preparation system (CAPS).  
148 Results are presented in the delta notation in ‰ relative to Vienna Pee Dee Belemnite  
149 (VPDB). Replicate analyses of an in-house standard are calibrated to NBS-19 and yield a  
150 routine external reproducibility of 0.065‰ for  $\delta^{18}\text{O}$  and 0.031‰  $\delta^{13}\text{C}$ .

#### 151 **2.5. Mg/Ca analysis**

152 Adhering clay particles were removed through ultrasonication in deionised water and  
153 methanol. Samples were then subject to first reductive then oxidative cleaning to remove  
154 ferromanganese oxide coatings and organic matter, respectively. Finally, the calcite tests  
155 were subjected to a weak acid “polish” to remove any re-absorbed ions (Boyle and Keigwin,  
156 1985; Hathorne, 2004; Rosenthal et al., 1997; Rosenthal et al., 1999).

157 Foraminiferal calcite was dissolved in 500 µl of 0.075 M  $\text{HNO}_3$ . An aliquot of this solution  
158 was diluted to give a concentration of approximately 3 ppm Ca. Samples were then analysed  
159 for Mg and Ca concentrations using a Perkin-Elmer Optima 4300 DV inductively coupled  
160 plasma – optical emission spectrometer (ICP-OES). The internal reproducibility of the  
161 Mg/Ca ratios, determined by 10 replicate analyses of five multi-element solutions, is <0.21%  
162 ( $1\sigma$ ; Greaves et al., 2008; Green et al., 2003).

### 163 **3. Results**

#### 164 **3.1. Inter-species stable isotope composition**

165 In Figure 3, we plot  $\delta^{18}\text{O}$  and  $\delta^{13}\text{C}$  for benthic and planktic foraminifera from each of our  
166 four study samples (Panels I through IV). The sizes of the data points are schematically  
167 representative of the size fraction of tests analysed. The planktic foraminifera fall into three  
168 distinct groups, (i) *G. bulloides*, “*G.*” *primordius*, and *G. altiapertura*, have low  $\delta^{18}\text{O}$  (~ -  
169 2‰) and high  $\delta^{13}\text{C}$  (~ +2.5‰), (ii) *C. dissimilis*, *C. ciperoensis*, and *C. indianus* form a group

170 with high  $\delta^{18}\text{O}$  ( $\sim +1\text{‰}$ ) and low  $\delta^{13}\text{C}$  values ( $\sim +1\text{‰}$ ), and (iii) *P. bella*, *P. siakensis/mayeri*,  
 171 and “*D.*” *venezuelana* (morphotype 1) display intermediate  $\delta^{18}\text{O}$  and  $\delta^{13}\text{C}$  values. Benthic  
 172 foraminifera yield the highest  $\delta^{18}\text{O}$  and lowest  $\delta^{13}\text{C}$  values of all.  $\delta^{13}\text{C}$  in *O. umbonatus* is  
 173 consistently  $\sim 1.5\text{‰}$  lower than in *C. mundulus*.  $\delta^{18}\text{O}$  in *G. bulloides* (a surface dweller in the  
 174 modern ocean) is 3.48 to 3.24‰ lower than the  $\delta^{18}\text{O}$  of *O. umbonatus*. The  $\delta^{18}\text{O}$  and  $\delta^{13}\text{C}$   
 175 values within each “*D.*” *venezuelana* morphotype vary by up to 0.9‰ and 0.5‰  
 176 respectively. Data for the three morphotypes plot within the same isotopic range as one  
 177 another both before (Figure 3 I') and after (Figure 3 IV') the Mi-1 event (Figure 1).

### 178 3.2. $\delta^{18}\text{O}$ , $\delta^{13}\text{C}$ , and Mg/Ca variation with test size

179 Figure 4 shows that, in general, in all three morphotypes of “*D.*” *venezuelana*,  $\delta^{18}\text{O}$  increases  
 180 with increasing test size in sample I (Figure 4b).  $\delta^{18}\text{O}$  values show no further increase above  
 181 the 355-400  $\mu\text{m}$  size fraction. Mg/Ca data for sample I show a trend similar to that seen in  
 182  $\delta^{18}\text{O}$  with values decreasing by  $>0.5$  mmol/mol across the size fraction range measured  
 183 (Figure 4d). A different distribution, however, is observed in  $\delta^{18}\text{O}$  and Mg/Ca with test size  
 184 in sample IV (Compare Figures 4a and c with 4b and d) where variation in  $\delta^{18}\text{O}$  and Mg/Ca  
 185 of “*D.*” *venezuelana* within a single size fraction is greater and no obvious trend in  $\delta^{18}\text{O}$  or  
 186 Mg/Ca is seen with test size.  $\delta^{13}\text{C}$  values are tightly grouped within individual size fractions  
 187 of all “*D.*” *venezuelana* morphotypes analysed both in sample I and sample IV (Figure 4e &  
 188 f). In both samples,  $\delta^{13}\text{C}$  increases with increasing test size by approximately 0.5‰ between  
 189 212 and 500  $\mu\text{m}$ .

## 190 4. Discussion

### 191 4.1. Inter and intra-specific calcification depths

192  $\delta^{13}\text{C}$  in foraminiferal test calcite is dependent on the isotopic signature of dissolved inorganic  
 193 carbon (DIC) in seawater. DIC is removed from seawater during primary production, and  $^{12}\text{C}$   
 194 is removed in preference to  $^{13}\text{C}$ . For this reason, the DIC in surface seawater is isotopically  
 195 “heavy”, whereas deep waters are isotopically “light” because of remineralisation of  $^{12}\text{C}$ -  
 196 enriched organic material (Kroopnick, 1985). Foraminiferal  $\delta^{13}\text{C}$  is affected by this and a  
 197 number of other processes that change as a function of depth, such as the photosynthetic  
 198 activity of symbionts, and irradiance levels (Spero and Williams, 1988; 1989).

199 The oxygen isotopic composition of ambient seawater ( $\delta^{18}\text{O}_{\text{sw}}$ ; controlled by ice volume and  
 200 salinity), and temperature of calcification are the primary controls on the  $\delta^{18}\text{O}$  of  
 201 foraminiferal calcite ( $\delta^{18}\text{O}_{\text{c}}$ ). Within individual samples at a given location in the ocean, the  
 202 most important effect on  $\delta^{18}\text{O}_{\text{c}}$  is temperature; calcification at lower temperatures producing

203 higher  $\delta^{18}\text{O}_c$  (Emiliani, 1955). The thermal gradient of the water column in tropical regions  
204 means that  $\delta^{18}\text{O}_c$  can change by as much as 4‰ between species that reside in the mixed  
205 layer and species that live deeper in the water column (Biolzi, 1983). Temperature changes  
206 most rapidly with depth through the thermocline, therefore, planktic foraminifera calcifying  
207 within the thermocline should record a greater change in  $\delta^{18}\text{O}$  than in  $\delta^{13}\text{C}$  with increasing  
208 depth (Pearson et al., 1993).

209 In this way, foraminiferal  $\delta^{18}\text{O}$  and  $\delta^{13}\text{C}$  can be used to assess the depth habitat of different  
210 species and morphotypes from our four samples (Figure 3 I to IV). The  $\delta^{18}\text{O}$  and  $\delta^{13}\text{C}$  values  
211 of benthic foraminifera are used to constrain temperature and  $\delta^{13}\text{C}$  in deep waters at this site,  
212 respectively.  $\delta^{13}\text{C}$  is lower in *O. umbonatus* than in *C. mundulus*, consistent with the view  
213 that *O. umbonatus*, in general, occupies a shallow infaunal niche below the sediment-water  
214 interface, whereas *C. mundulus* calcifies epifaunally (Rathburn and Corliss, 1994). Our stable  
215 isotope data for planktic foraminifera shown in Figure 3 indicate that *G. bulloides*, “*G.*”  
216 *primordius*, and *G. altiapertura* are surface dwellers (lowest  $\delta^{18}\text{O}$  and highest  $\delta^{13}\text{C}$ ), *P. bella*  
217 and *P. siakensis/mayeri* are thermocline dwellers, and *C. dissimilis*, *C. ciproensis*, and *C.*  
218 *indianus* are sub-thermocline dwellers (highest  $\delta^{18}\text{O}$  and lowest  $\delta^{13}\text{C}$ ).

219 Our  $\delta^{18}\text{O}$  and  $\delta^{13}\text{C}$  data for “*D.*” *venezuelana* morphotype 1 suggest that this taxon calcified  
220 in the lower thermocline in all four samples spanning the O/M boundary at Ceara Rise  
221 (Figure 3 I to IV), with no indication of calcification in the mixed layer, as observed in the  
222 equatorial Pacific and Gulf of Mexico (Poore and Matthews, 1984; Wade et al., 2007). Our  
223 inferred lower thermocline depth habitat for “*D.*” *venezuelana* is consistent with the limited  
224 data previously available from O/M boundary sediments in the equatorial Atlantic (Biolzi,  
225 1983; Pearson et al., 1997; Pearson and Wade, 2009). This observation prompts us to  
226 question whether the variation in inferred calcification depth of “*D.*” *venezuelana* in the  
227 literature (Figure 2) is a geographical or temporal phenomenon. We note that studies of  
228 material pre-dating the mid-Oligocene assign a surface water habitat to “*D.*” *venezuelana*  
229 (Poore and Matthews, 1984; Wade et al., 2007), whereas analyses of material of mid-  
230 Miocene or younger age report a deep-water calcification depth for “*D.*” *venezuelana*  
231 (Barrera et al., 1985; Hodell and Vayavananda, 1993; Keller, 1985; Norris et al., 1993;  
232 Pearson et al., 2001; Pearson and Shackleton, 1995; Smart and Thomas, 2006). Taken  
233 together with our new results, this observation suggests that “*D.*” *venezuelana* has changed  
234 its depth habitat over time. A habitat shift such as this has also been invoked to explain a  
235 mid-Oligocene (~27 Ma) increase in the  $\delta^{18}\text{O}$  time series of “*D.*” *venezuelana* in the absence  
236 of an associated shift in benthic  $\delta^{18}\text{O}$  (Wade and Pälike, 2004). A study of O/M boundary



237 planktic foraminifera in the Indian Ocean reports a lowermost thermocline to sub-thermocline  
 238 depth habitat for “*D.*” *venezuelana* (Spezzaferri and Pearson, 2009), which in conjunction  
 239 with previous studies and our new data suggests that the transition from a surface to a sub-  
 240 thermocline habitat was complete shortly after the early Miocene. Changes in preferred  
 241 calcification depth of planktic foraminifera are not uncommon on long (geological)  
 242 timescales; taxa are reported to have shifted habitat both up (e.g. Coxall et al., 2000; Coxall  
 243 et al., 2007) and down (e.g. Norris et al., 1993) the water column through time.

244 In our dataset,  $\delta^{18}\text{O}$  and  $\delta^{13}\text{C}$  fall within the same range for all three morphotypes of “*D.*”  
 245 *venezuelana* (Figure 3 I' and IV'), implying the same (lower thermocline) depth habitat. This  
 246 consistency is true for samples from both the upper Oligocene (I) and the lower Miocene  
 247 (IV). The close similarity in inferred calcification depth for all three morphotypes strongly  
 248 suggests that they need not be separated where large samples are required (e.g., to generate  
 249 palaeoceanographic records of silicate weathering using Nd and Li isotope methods).

## 250 4.2. Geochemical changes with ontogeny

### 251 4.2.1 Late Oligocene (Sample I)

252 In our upper Oligocene sample there is tight grouping of  $\delta^{18}\text{O}$  and Mg/Ca within each size  
 253 fraction of “*D.*” *venezuelana*, for all three morphotypes (Figure 4b and d). These data  
 254 suggest that smaller “*D.*” *venezuelana* calcify under the warmest conditions, higher in the  
 255 water column, while intermediate to larger individuals calcify in slightly deeper, cooler  
 256 waters.

257 The covariation in Mg/Ca and  $\delta^{18}\text{O}$  within sample I implies that temperature is the dominant  
 258 control on  $\delta^{18}\text{O}_c$ , given the strong temperature dependence of Mg/Ca in planktic foraminiferal  
 259 calcite (Anand et al., 2003; Elderfield and Ganssen, 2000). The temperature of calcification  
 260 can be estimated from Mg/Ca as follows, using the multispecies calibration of Anand et al.  
 261 (2003),

$$262 \quad \text{Mg/Ca}_{\text{foram}} = 0.38 \exp(0.090 \cdot T) \quad (1)$$

263 where T is temperature ( $^{\circ}\text{C}$ ) and  $\text{Mg/Ca}_{\text{foram}}$  is the Mg/Ca of foraminiferal calcite, reported in  
 264 mmol/mol. Using this equation we calculate calcification temperatures for “*D.*” *venezuelana*  
 265 in our upper Oligocene sample ranging from  $\sim 20$  to  $\sim 22$   $^{\circ}\text{C}$ . It is important to note that,  
 266 although Equation 1 is generally applicable to all modern planktic foraminifera species, the  
 267 values of the constants are species specific (Anand et al., 2003). “*D.*” *venezuelana* is an  
 268 extinct taxa, so we cannot evaluate directly the extent to which these constants are  
 269 appropriate. However, substituting the constants in Equation 1 with those determined for

270 *Neogloboquadrina dutertrei*, a modern thermocline-dwelling species, yields Mg/Ca  
 271 temperatures that are only about 1 °C warmer. A more important source of uncertainty in  
 272 absolute temperatures is that Equation 1 assumes the Mg/Ca ratio of seawater of the Oligo-  
 273 Miocene is the same as it is today, while numerous lines of evidence suggest that the Mg/Ca  
 274 ratio of seawater has increased over the Cenozoic (Broecker and Yu, 2011; Coggon et al.,  
 275 2010; Dickson, 2002; Hardie, 1996; Stanley and Hardie, 1998; Tyrrell and Zeebe, 2004;  
 276 Wilkinson and Algeo, 1989). Assuming that seawater Mg/Ca was lower in the late Oligocene  
 277 than today, failure to adjust for this factor yields artificially cool calcification temperatures.  
 278 We evaluate this effect by adjusting the pre-exponent (*cf.* Lear et al., 2000) of the Anand et  
 279 al., (2003) temperature equation as follows,

$$280 \qquad \qquad \qquad \qquad \qquad \qquad \qquad \qquad \qquad \qquad \qquad \qquad \qquad (2)$$

281 where  $Mg/Ca_{sw}$  is the Mg/Ca composition of modern seawater (~5.17 mol/mol) and  $Mg/Ca_{sw-OM}$   
 282 is the estimated Mg/Ca composition of the ocean at O/M boundary time. Estimates of the  
 283 secular shifts in oceanic Mg/Ca composition yield  $Mg/Ca_{sw-OM}$  values ranging from 2  
 284 mol/mol (Coggon et al., 2010) to 4 mol/mol (Wilkinson and Algeo, 1989). Using this range  
 285 of  $Mg/Ca_{sw-OM}$  estimates in Equation 2, calcification temperatures of “*D.*” *venezuelana*  
 286 increase by 3 to 9 °C compared to our original estimates, but the temperature offset between  
 287 size fractions does not change.

288 The temperature of calcification can also be estimated from  $\delta^{18}O$ . We use the temperature  
 289 calibration for the modern planktic foraminifera *Orbulina universa* (low light) from Bemis et  
 290 al., (1998),

$$291 \qquad \qquad \qquad T \text{ (}^\circ\text{C)} = 16.5 - 4.8 (\delta^{18}O_c - \delta^{18}O_{sw}) \qquad \qquad \qquad (3)$$

292 where  $\delta^{18}O_{sw}$  for late Oligocene time is assumed to be -0.5‰ (Lear et al., 2004). Applying  
 293 Equation 3 to our data, we obtain calcification temperatures for “*D.*” *venezuelana* that are, on  
 294 average, ~ 4°C lower than corresponding Mg/Ca-derived temperatures.  $\delta^{18}O$  temperature  
 295 calibrations are also species specific and the use of a temperature calibration for the modern  
 296 planktic foraminifera *G. bulloides* (Bemis et al., 2000) yields  $\delta^{18}O$  temperatures for “*D.*”  
 297 *venezuelana* that are a further 3°C lower but, once again, the range of temperatures calculated  
 298 using  $\delta^{18}O_c$  is not sensitive to choice of calibration. Discrepancy between  $\delta^{18}O$ - and Mg/Ca-  
 299 derived estimates of absolute temperature is not unexpected in planktic foraminifera with a  
 300 “frosty” taphonomy such as those from ODP Site 925, because of the apparently greater  
 301 susceptibility of  $\delta^{18}O_c$  to diagenetic alteration on the sea floor compared to Mg/Ca (Sexton et

302 al., 2006). Yet the range of calcification temperatures calculated for all morphotypes of “*D.*”  
303 *venezuelana* (2-3°C) across all size fractions in our upper Oligocene sample is similar to that  
304 calculated from Mg/Ca.

305 The thermocline of the modern Ceara Rise exhibits negligible seasonal variation in depth and  
306 has a maximum temperature gradient of 1.3°C per 10 m increase in water depth (Levitus and  
307 Boyer, 1994). Our calculated 2 to 3°C range in calcification temperature, estimated using two  
308 independent temperature proxies, is very consistent with findings of previous studies (Nathan  
309 and Leckie, 2009; Wade et al., 2007) and suggests that “*D.*” *venezuelana* migrates vertically  
310 downwards in the water column during its life cycle by up to 20 m. We conclude, therefore,  
311 that the anomalously low  $\delta^{18}\text{O}$  value of “*D.*” *venezuelana* recorded in the equatorial Pacific  
312 may at least in part result from, as suggested by Wade et al., (2007), the use of the smaller  
313 and restricted, 300-355  $\mu\text{m}$  size fraction.

#### 314 4.2.2 Early Miocene (Sample IV)

315 Our data show greater spread in  $\delta^{18}\text{O}$  and Mg/Ca in the early Miocene (Figure 4a & c) than is  
316 the case for the late Oligocene, with no consistent pattern of change with test size. We  
317 consider two potential explanations to account for these observations; firstly, poorer sample  
318 preservation in the early Miocene, and secondly, instability of the tropical Atlantic  
319 thermocline in the early Miocene.

320 At low latitudes, in general, planktic  $\delta^{18}\text{O}$  increases during post-depositional alteration  
321 because of the steep vertical oceanic temperature gradient, however Mg/Ca can either  
322 increase or decrease depending on the partition coefficients of Mg into biogenic vs. inorganic  
323 calcite (Sexton et al., 2006). We note four lines of evidence that suggest that our Oligocene  
324 versus Miocene results in test  $\delta^{18}\text{O}$  and Mg/Ca are not attributable to the diagenetic histories  
325 of the samples analysed. (i) During our examination of ODP Site 925 material under the  
326 binocular light microscope we observed no discernable taphonomic offset between material  
327 of late Oligocene and early Miocene age. (ii) The preservation of “*D.*” *venezuelana* in both  
328 samples can also be assessed by scanning electron microscope (SEM) analysis of test wall  
329 textures. Plate 3 shows that tests from both samples have been subject to recrystallisation,  
330 and can be considered to exhibit “frosty” taphonomy in the nomenclature of Sexton et al.,  
331 (2006). Test architecture at the micron scale has been obscured by cemented overgrowths of  
332 inorganic calcite; however, the coarse cancellate wall structure is still visible in all of the tests  
333 examined. The degree of surface recrystallisation is shown to be similar in both samples. (iii)  
334 Cross sections through the test wall are shown in Plate 4. A distinctive layer, marking the  
335 original position of the primary organic membrane (POM), the site of initial calcification, is

336 still visible in all specimens. Post depositional precipitation of inorganic calcite inside tests  
337 has the potential to obscure primary shell chemistry. However, we find the extent to which  
338 this internal recrystallisation has taken place to be no more pronounced in our lower Miocene  
339 sample (Plate 4 IV a-e) than in our upper Oligocene sample (Plate 4 I a-e). (iv) Oligocene and  
340 Miocene age ODP cores from Ceara Rise exhibit changes in calcium carbonate content that  
341 are linked to inferred glacial-interglacial cycles. Glacial intervals, characterised by high  
342 benthic  $\delta^{18}\text{O}$  (Pälike et al., 2006a; Zachos et al., 2001), coincide with peaks in magnetic  
343 susceptibility and low colour reflectance. These dark bands result from carbonate dissolution  
344 and contain poorer preserved microfossils (Shipboard Scientific Party, 1995a). Based on  
345 colour reflectance data, calibrated versus low-resolution weight percent calcium carbonate,  
346 we estimate the carbonate content of our upper Oligocene and lower Miocene samples to be,  
347 respectively, 61% and 63%; a feature that, along with our other observations, suggests  
348 preservation between samples is comparable.

349 We also consider the possibility that the different ontogenetic results that we obtain for  $\delta^{18}\text{O}$   
350 and Mg/Ca in our Oligocene versus Miocene samples are attributable to instability in the  
351 tropical Atlantic thermocline in the early Miocene. Global coupled climate models suggest  
352 that there were considerable changes in ocean circulation from the late Oligocene to the early  
353 Miocene, including a flow reversal through the Central American Seaway (CAS) that bathed  
354 the Caribbean Sea and western equatorial Atlantic in cooler, less saline Pacific waters  
355 (Bernsen and Dijkstra, 2010; von der Heydt and Dijkstra, 2005; von der Heydt and Dijkstra,  
356 2006). In these simulations, the persistence of eastern equatorial winds maintains a westward  
357 flow of uppermost surface waters forcing the bulk of the newly induced eastern flow through  
358 the CAS to occur at depths of 100m (von der Heydt and Dijkstra, 2005; von der Heydt and  
359 Dijkstra, 2006). Input of Pacific waters, sourced from seasonal upwelling zones, is thought to  
360 have reduced the surface temperature of the tropical equatorial Atlantic by more than 1 °C  
361 (von der Heydt and Dijkstra, 2005). Given the depth of flow, upwelling source, and  
362 magnitude of cooling induced by the Pacific waters entering the Atlantic Ocean during the  
363 early Miocene it is reasonable to expect seasonal shifts in the thermocline at Ceara Rise that  
364 might act to help obscure systematic variations in  $\delta^{18}\text{O}$  and Mg/Ca of "*D.*" *venezuelana* with  
365 test size. Species inhabiting the tropics exhibit little seasonal variation in calcification rate  
366 (Kucera et al., 2007) allowing "*D.*" *venezuelana*, with its high geochemical sensitivity to  
367 changes in vertical temperature regime, to capture such intra-annual temperature variation.  
368 High variability of stable isotope data in "*D.*" *venezuelana*, relative to other planktic  
369 foraminifera, is also reported in mid-Miocene samples from the western equatorial Pacific,  
370 for which similar thermocline instability is invoked (Nathan and Leckie, 2009). If our

371 interpretation is correct, then the potentially implied changes in ocean circulation will have  
372 important implications for some silicate weathering proxies, particularly those with short  
373 ocean residence times, such as neodymium.

#### 374 **4.3. Symbiont palaeoecology**

375 Steep carbon isotopic gradients with increasing planktic foraminiferal test size are generally  
376 associated with photosymbiont activity, specifically of dinoflagellates, whereas shallow  
377 gradients are more commonly associated with asymbiotic or chrysophyte symbiont-bearing  
378 species (Bornemann and Norris, 2007; D'Hondt et al., 1994; Elderfield et al., 2002; Pearson  
379 et al., 1993; Spero and Williams, 1988). To investigate the potential footprint of  
380 photosymbionts in our "*D.*" *venezuelana* specimens, we compare our multiple size fraction  
381  $\delta^{13}\text{C}$  data in Figure 4e and f to similar data from known photosymbiont bearing and  
382 asymbiotic planktic foraminifera recovered from modern core-tops at two western equatorial  
383 Atlantic sites (Ravelo and Fairbanks, 1995). We normalise these core-top  $\delta^{13}\text{C}$  data by  
384 matching the y-intercept of each line of best fit to that of our "*D.*" *venezuelana*  $\delta^{13}\text{C}$  results  
385 from sample I and sample IV. This exercise allows us to adjust for temporal changes in  
386 oceanic  $\delta^{13}\text{C}$  (Figure 1) and thereby isolate the  $\delta^{13}\text{C}$  gradient. Solid red lines in Figure 4e & f  
387 depict the steeper  $\delta^{13}\text{C}$  gradients ( $\Delta\delta^{13}\text{C}/100\ \mu\text{m} > 0.2\text{‰}$ ) of known photosymbiont bearing  
388 planktic foraminifera, whereas the dashed black lines show the more modest gradients  
389 ( $\Delta\delta^{13}\text{C}/100\ \mu\text{m} < 0.2\text{‰}$ ) of living asymbiotic taxa. These data describe a continuum of  
390 gradients rather than two completely distinct populations presumably reflecting other  
391 influences on test  $\delta^{13}\text{C}$  (e.g. physiological effects or symbiont type) that sometimes make the  
392 application of this approach to fossil taxa less than straightforward (e.g. Bornemann and  
393 Norris, 2007; Norris, 1998; Norris and Wilson, 1998).

394 The shallow  $\delta^{13}\text{C}$  gradient that we document in the Miocene for sample I lies within the zone  
395 of known modern asymbiotic taxa while the data for sample IV fall on the dividing line  
396 between modern asymbiotic and dinoflagellate-bearing taxa. The only moderate enrichment  
397 of  $^{13}\text{C}$  in larger "*D.*" *venezuelana* specimens, along with its inferred lower thermocline depth  
398 habitat, implies that this species is asymbiotic (rather than hosting chrysophyte symbionts)  
399 similar to many Oligocene planktic foraminifera (Wade et al., 2008).

#### 400 **5. Conclusions and Implications**

401 The planktic foraminifera species "*D.*" *venezuelana* appears to have calcified within the  
402 lower thermocline during the late Oligocene and the early Miocene at Ceara Rise in the  
403 western equatorial Atlantic. This means that variations in the chemical composition of the

404 tests over this interval should reflect environmental changes in ocean chemistry, rather than  
405 changes in depth habitat. However, over longer time periods (tens of millions of years), “*D.*”  
406 *venezuelana* appears to have shifted its depth of calcification from surface waters, to  
407 thermocline (during the late Oligocene to early Miocene), to sub-thermocline waters. This  
408 secular change from surface to deep-water depth habitat must be taken into consideration  
409 when interpreting long-term records. For example, Li/Ca ratios in planktic foraminifera may  
410 be, in part, regulated by the carbonate ion concentration  $[\text{CO}_3^{2-}]$  of seawater (Hall and Chan,  
411 2004).  $[\text{CO}_3^{2-}]$  decreases with depth in the oceans, therefore a change in calcification depth of  
412 “*D.*” *venezuelana* from the early Oligocene to late Miocene may act to amplify or dampen  
413 changes in the Li concentration of seawater.

414 Detailed analyses of  $\delta^{18}\text{O}$ ,  $\delta^{13}\text{C}$  and Mg/Ca in different size fractions, in conjunction with  
415 previous studies, reveal that, in the late Oligocene, “*D.*” *venezuelana* shows ontogenetic  
416 variations in its depth habitat with younger specimens calcifying high in the water column  
417 followed by a descent to deeper calcification depths in the later stages of development. We  
418 therefore recommend the use of the large,  $>355\ \mu\text{m}$ , size fraction for the purposes of  
419 generating geochemical time-series records (e.g. Nathan and Leckie, 2009). These  
420 ontogenetic changes are not evident in our early Miocene data, possibly indicating instability  
421 of the Miocene thermocline.

422 Finally, we have distinguished three morphotypes of “*D.*” *venezuelana* in this study, which  
423 all appear to have the same palaeoecology. It remains important to separate these  
424 morphotypes from species that share morphological similarities, such as *D. globosa* and *D.*  
425 *altispira*, that were lower mixed layer or upper thermocline dwellers, (e.g. Gasperi and  
426 Kennett, 1993; Hodell and Vayavananda, 1993; Pearson and Shackleton, 1995), yet our  
427 finding that different morphotypes of “*D.*” *venezuelana* are palaeoecologically inseparable is  
428 good news for geochemical proxy techniques that rely on the availability of unusually large  
429 samples of mono-specific foraminiferal calcite.

430

## 431 **6. List of species**

### 432 **Planktic foraminifera**

433 *Catapsydrax ciperensis* (Cushman and Bermúdez, 1937)

434 *Catapsydrax dissimilis* (Cushman and Bermúdez, 1937)

435 *Catapsydrax indianus* Spezzaferri and Pearson, 2009

436 *"Dentoglobigerina" venezuelana* (Hedberg, 1937); see Pearson and Wade (2009) for further  
437 details.

438 *Globigerina bulloides* d'Orbigny, 1926

439 *Globigerinoides altiapertura* Bolli, 1957

440 "*Globigerinoides*" *primordius* Blow and Banner, 1962

441 *Paragloborotalia bella* (Jenkins, 1967)

442 *Paragloborotalia siakensis/mayeri* (LeRoy, 1939/Cushman and Ellisor, 1939)

443 **Benthic foraminifera**

444 *Cibicidoides mundulus* (Brady, Parker, and Jones, 1888)

445 *Oridorsalis umbonatus* (Reuss, 1851)

446 **Table 1:** Sample details. ODP sample identification given as Leg, Site, Hole, Core and  
447 Interval (cm). Magnetochron assignment is based on correlation to Site 1090. Ages are  
448 estimated using the Site 926 age model (Pälike et al., 2006a).

Sample #	ODP sample identification	Site 925 depth (mbsf)	Equivalent site 926 depth (mcd)	Inferred magnetochron	Age (Ma)
IV	154-925A-20R-2W, 130–132 cm	470.60	439.83	Base C6Ar	21.0
III	154-925A-22R-4W, 10–12 cm	491.70	488.27	Top C6Cn.1n	22.6
II	154-925A-22R-7W, 30–32 cm	496.40	492.26	Middle C6Cn.1n	22.7
I	154-925A-24R-1W, 110–112 cm	507.40	530.54	Top C7Bn.2n	24.2

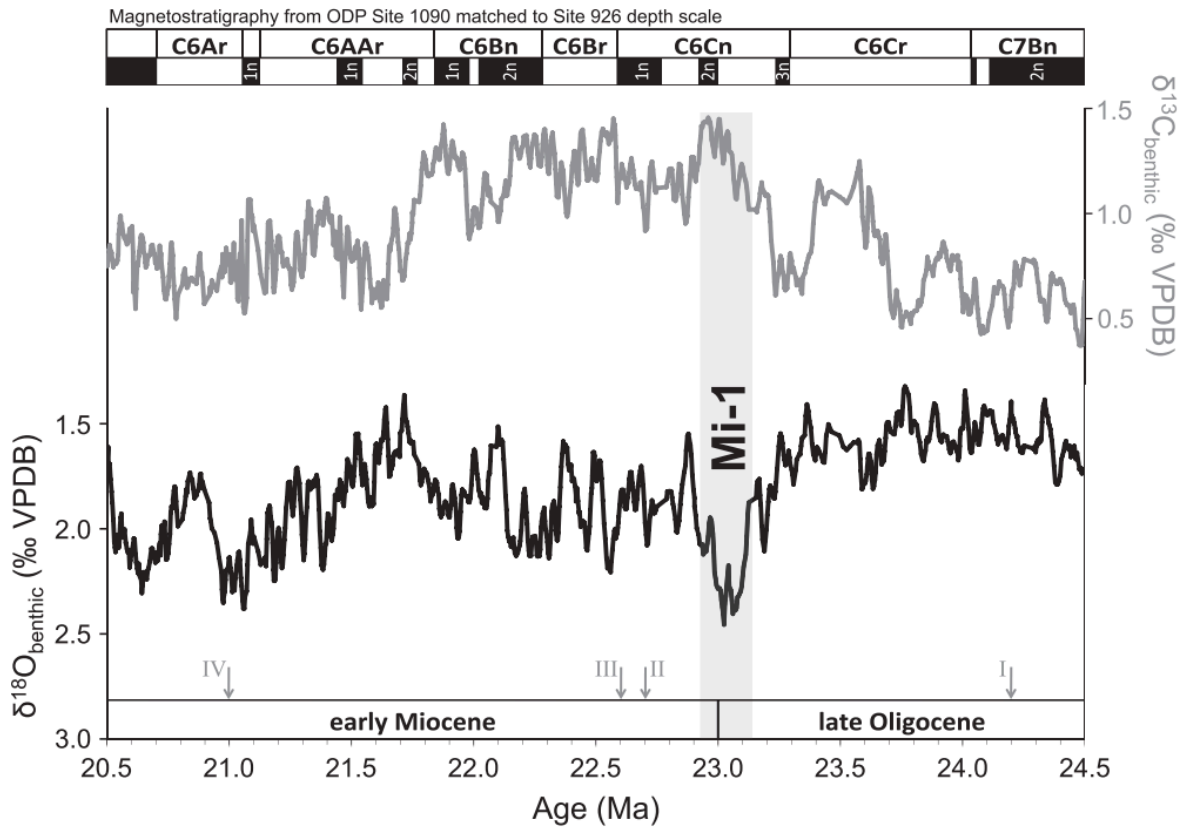
449

450

451

452

453

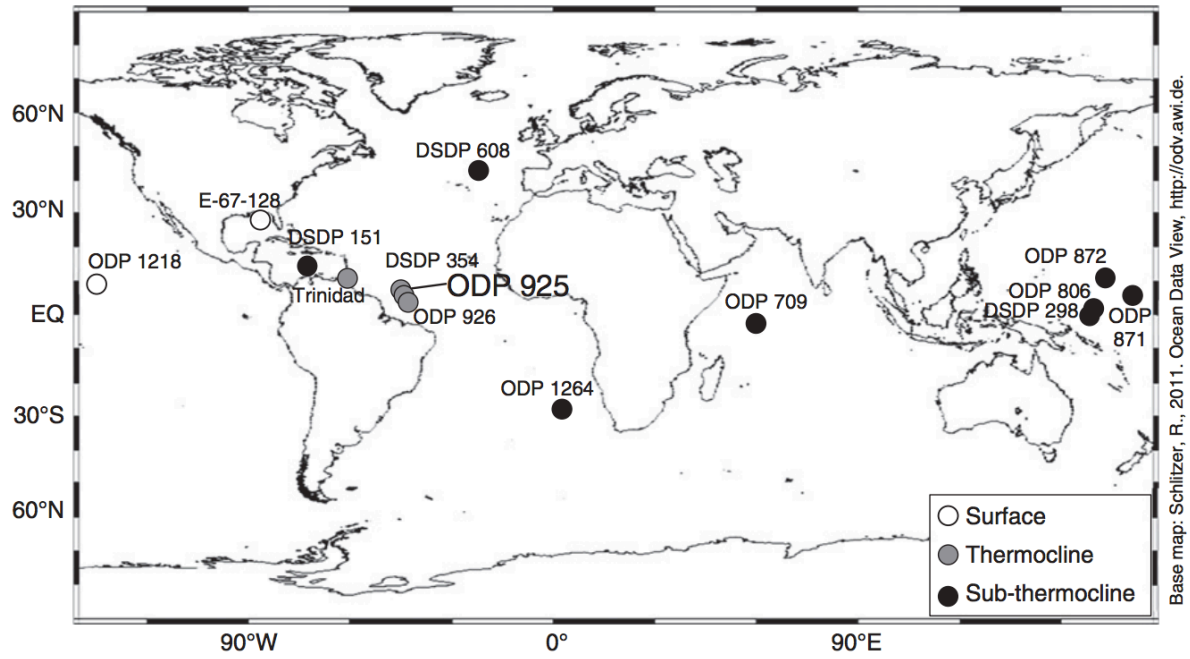


454

455 **Figure 1:** Benthic foraminiferal stable isotope records across the Oligocene-Miocene  
 456 boundary from ODP Site 926 (Pälike et al., 2006a). Solid black and grey lines show a 5-point  
 457 moving average of  $\delta^{18}\text{O}$  and  $\delta^{13}\text{C}$ , respectively. Vertical grey bar highlights the Mi-1  
 458 excursion (Miller et al., 1991; Zachos et al., 2001). Grey arrows denote stratigraphic position  
 459 of samples investigated in this study (I-IV). Magnetostratigraphy from ODP Site 1090, South  
 460 Atlantic (Billups et al., 2002; Channell et al., 2003), correlated to Site 926 depth scale  
 461 (Liebrand et al., 2011), and matched through shipboard physical property data to Site 925  
 462 depth scale.

463





464

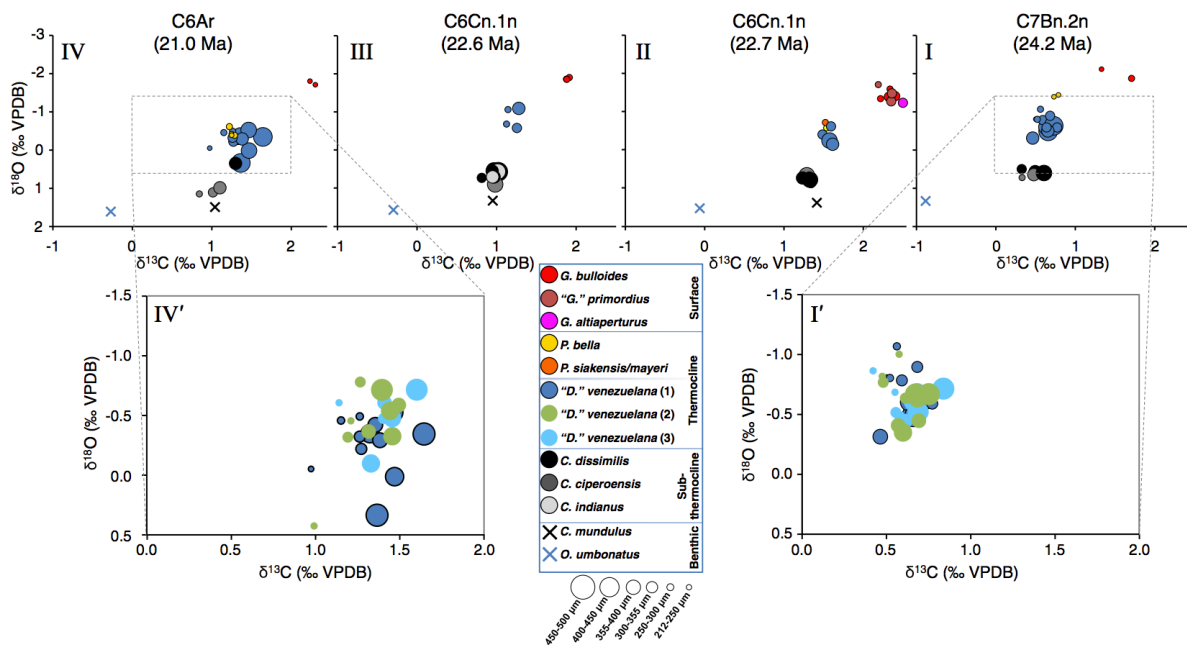
465 **Figure 2:** Location of ODP Site 925 in the equatorial Atlantic Ocean. Also shown are other  
 466 core sites for which the depth habitat (surface, thermocline or sub-thermocline) of “*D.*”  
 467 *venezuelana* has been inferred from foraminiferal  $\delta^{18}\text{O}$  and  $\delta^{13}\text{C}$  (Biolzi, 1983; Hodell and  
 468 Vayavananda, 1993; Norris et al., 1993; Pearson et al., 2001; Pearson et al., 1997; Pearson  
 469 and Wade, 2009; Poore and Matthews, 1984; Smart and Thomas, 2006; Wade et al., 2007).

470

471

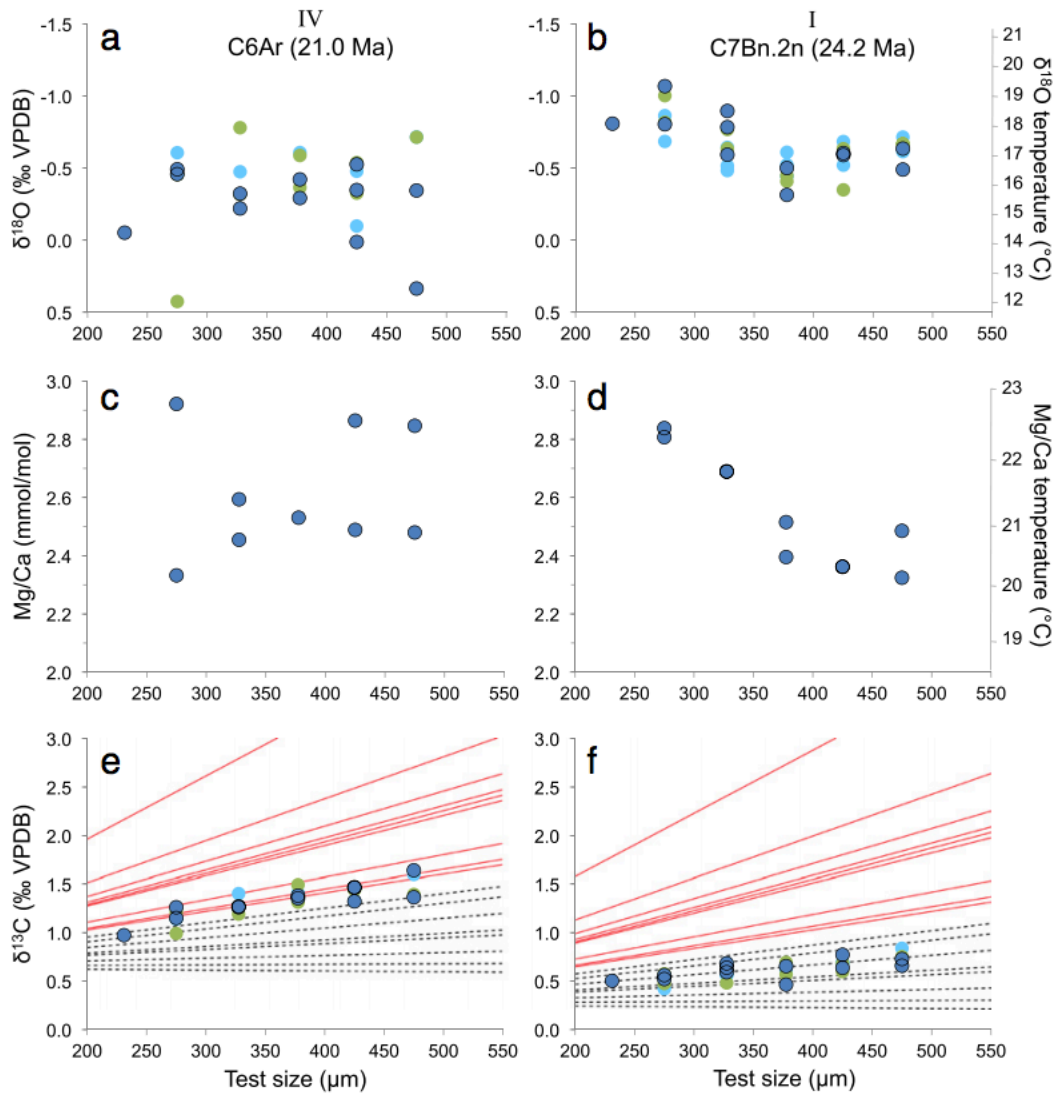
472

473



474

475 **Figure 3:**  $\delta^{18}\text{O}$  and  $\delta^{13}\text{C}$  in foraminiferal calcite recovered from ODP Site 925. The four  
 476 samples (I – IV) span the O/M boundary. I' and IV' are enlarged sections of plots I and IV  
 477 showing all "*D.* venezuelana" morphotypes (morphotype 1 in dark blue, morphotype 2 in  
 478 green and morphotype 3 in light blue). The colour and the size of the symbol schematically  
 479 represent the species and the size fraction.



480

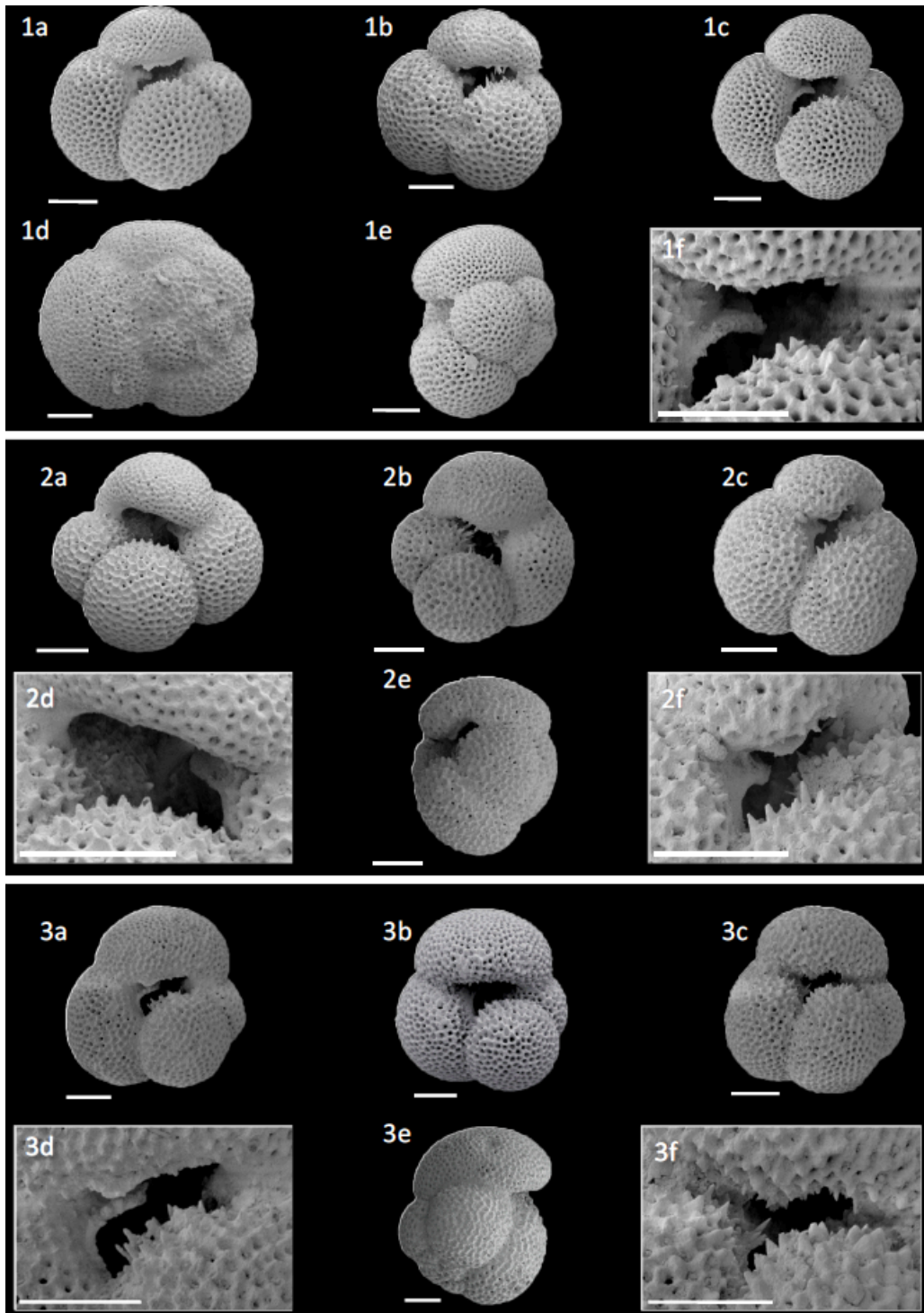
481 **Figure 4:** Changes in  $\delta^{18}\text{O}$ ,  $\delta^{13}\text{C}$  and Mg/Ca with test size of “*D.*” *venezuelana*. Morphotype  
 482 1 (dark blue circles), 2 (green circles) and 3 (light blue circles). Mg/Ca temperature is derived  
 483 from an “all species” calibration (Equation 1; Anand et al., 2003).  $\delta^{18}\text{O}$  temperature is  
 484 derived from Equation 3 (Bemis et al., 1998). Temperature scales apply only to Panels b and  
 485 d (sample I) and *not* to Panels a and c (see text for details). Lines in Panels e and f represent  
 486 the  $\delta^{13}\text{C}$  gradients of modern symbiotic (solid red lines; *Globigerinoides ruber* (both pink and  
 487 white), *Globigerinoides aequilateralis*, *Globigerinoides sacculifer* (both with and without  
 488 sac), *Neogloboquadrina dutertrei*, *Globigerinoides conglobatus*, and *Orbulina universa*) and  
 489 asymbiotic planktic foraminifera (black dashed lines; *Globorotalia menardii*, *Globorotalia*  
 490 *truncatulinoidea*, *Pulleniatina obliquiloculata*, *Globorotalia crassaformis*, *Globorotalia*  
 491 *tumida*) from two western equatorial Atlantic sites (Ravelo and Fairbanks, 1995).

492

493

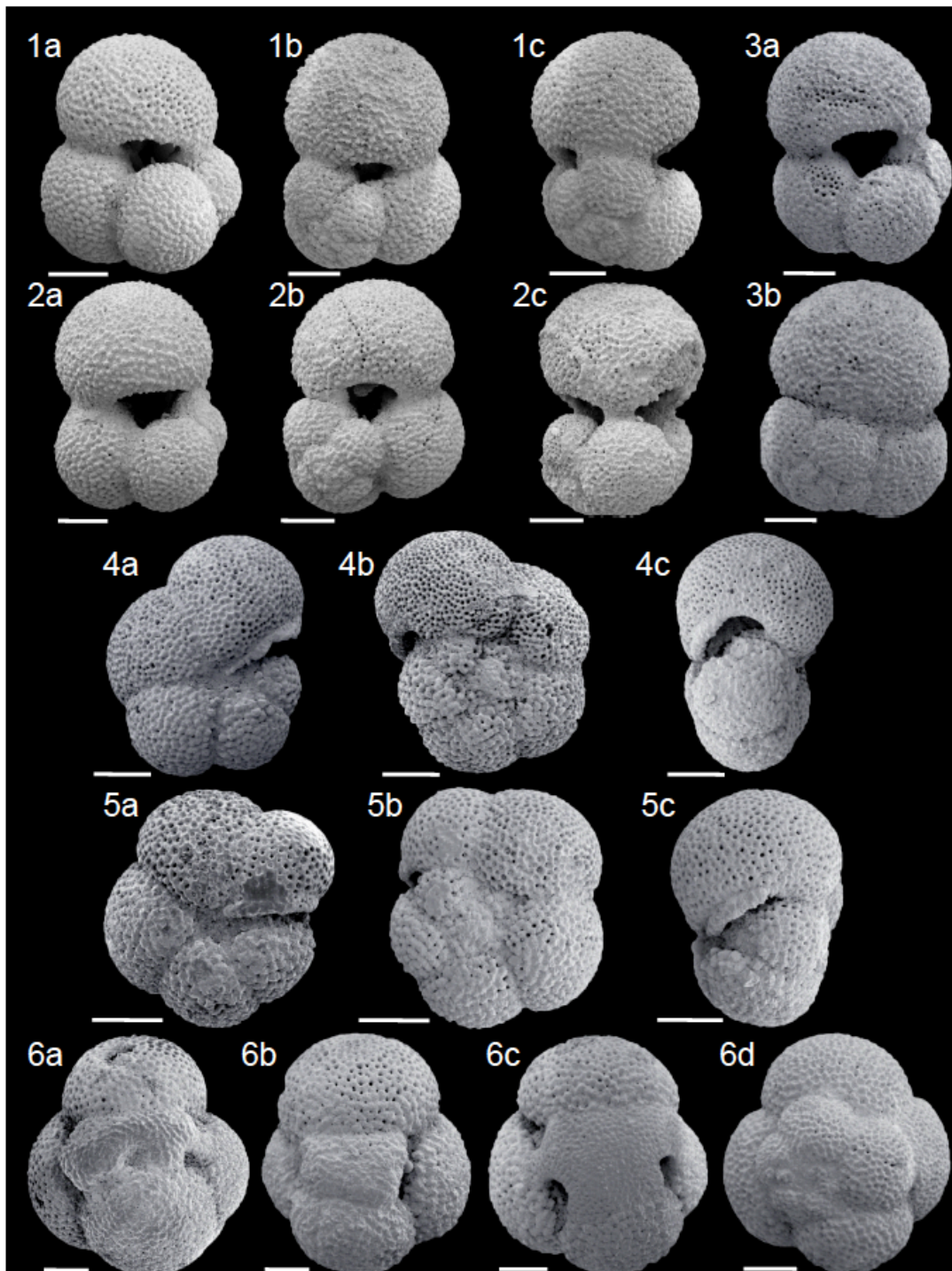
494

495



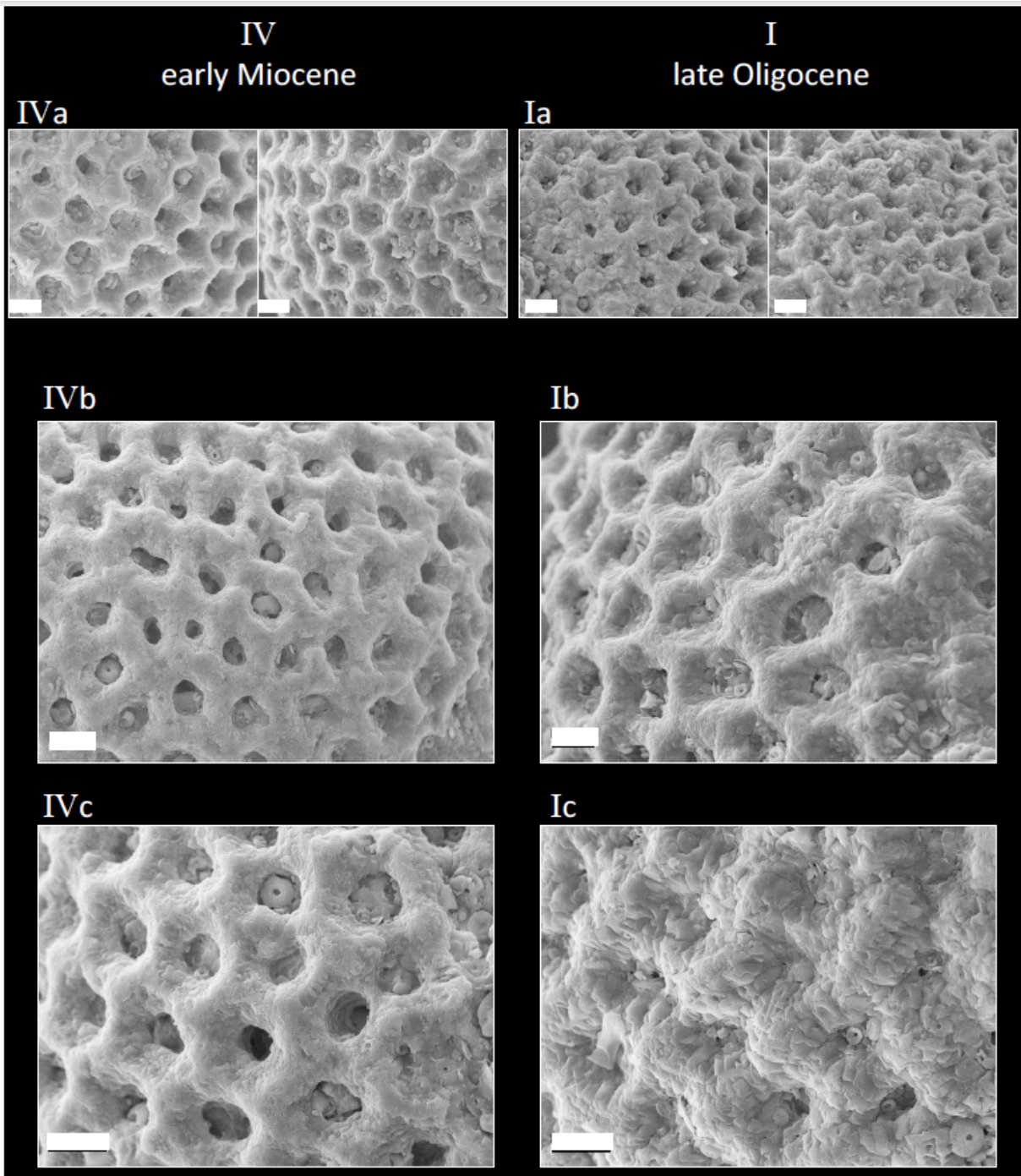
496

497 **Plate 1:** Scanning electron microscope images of *Dentoglobigerina* *venezuelana*  
 498 morphotypes from ODP Site 925. All scale bars are 100  $\mu\text{m}$ . **1(a-f).** "*D.*" *venezuelana*  
 499 morphotype 1, **1(a-c)**. Umbilical views, 154-925A-24R-5W, 22-24 cm, **1d**. Spiral view, 154-  
 500 925A-22R-7W, 30-32 cm, **1e**. Side view of specimen 1c, **1f**. Detailed wall texture and  
 501 apertural view of specimen 1c. **2(a-f).** "*D.*" *venezuelana* morphotype 2 (low arched  
 502 aperture), **2(a-c)**. Umbilical views, 154-925A-24R-5W, 22-24 cm, **2d**. Detailed wall texture  
 503 and apertural view of specimen 2a, **2e**. Side view of specimen 2c, **2f**. Detailed wall texture  
 504 and apertural view of specimen 2c, **3(a-f)**. "*D.*" *venezuelana* morphotype 3 (large final  
 505 chamber), **3(a-c)**. Umbilical views, 154-925A-24R-5W, 22-24 cm, **3d**. Detailed wall texture  
 506 and apertural view of specimen 3a, **3e**. Side view, 154-925A-22R-7W, 30-32 cm, **3f**. Detailed  
 507 wall texture and apertural view of specimen 3c.



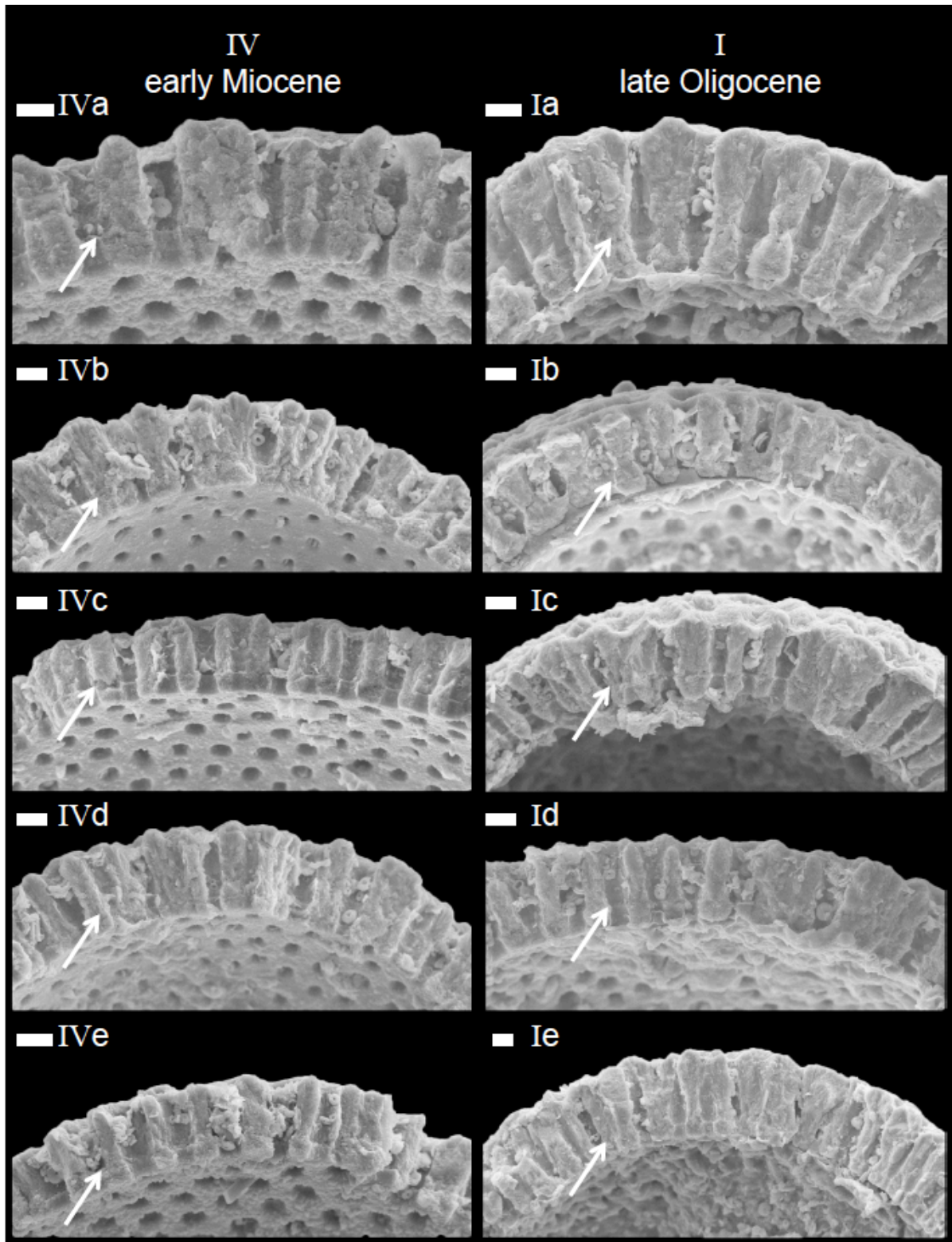
508

509 **Plate 2:** Scanning electron microscope images of Oligocene and Miocene planktic  
 510 foraminifera from ODP Site 925 illustrating species concepts adopted in this study. All scale  
 511 bars are 100  $\mu\text{m}$ . **1(a-c).** *Globigerinoides primordius*, 154-925A-22R-7W, 30-32 cm, **1a.**  
 512 Umbilical view, **1b.** Spiral view, **1c.** Side view, **2(a-c).** *Globigerinoides altiaperturaus*, 154-  
 513 925A-22R-7W, 30-32 cm, **2a.** Umbilical view, **2b.** Spiral view, **2c.** Side view, **3(a-b).**  
 514 *Globigerina bulloides*, 154-925A-22R-7W, 30-32 cm, **3a.** Umbilical view, **3b.** Spiral view,  
 515 **4(a-c).** *Paragloborotalia siakensis/mayeri*, 154-925A-22R-7W, 30-32 cm, **4a.** Umbilical  
 516 view, **4b.** Spiral view, **4c.** Side view, **5(a-c).** *Paragloborotalia bella*, 154-925A-22R-7W, 30-  
 517 32 cm, **5a.** Umbilical view, **5b.** Spiral view, **5c.** Side view, **6a.** *Catapsydrax indianus*,  
 518 umbilical view, 154-925A-22R-4W, 10-12 cm, **6b.** *Catapsydrax dissimilis*, umbilical view,  
 519 154-925A-22R-7W, 30-32 cm, **6c.** *Catapsydrax ciperoensis*, umbilical view, 154-925A-22R-  
 520 7W, 30-32 cm, **6d.** *Catapsydrax dissimilis*, spiral view, 154-925A-22R-7W, 30-32 cm.



521

522 **Plate 3:** Scanning electron microscope images of "*D.*" *venezuelana* morphotype 1 wall  
 523 textures from samples I (upper Oligocene) and IV (lower Miocene). All scale bars are 10 μm.



524

525 **Plate 4:** Scanning electron microscope images of "*D.*" *venezuelana* morphotype 1 wall cross  
 526 sections. All scale bars are 10  $\mu\text{m}$ . White arrows show the original position of the primary  
 527 organic membrane. **IV(a-e).** Test cross section images of "*D.*" *venezuelana* from five  
 528 different specimens in sample IV (lower Miocene). **I(a-e).** Test cross section images of "*D.*"  
 529 *venezuelana* from five different specimens in sample I (upper Oligocene).

530

531

532

533 **Acknowledgements**

534 This work used samples provided by the Ocean Drilling Program (ODP). The ODP (now  
535 IODP) is sponsored by the US National Science Foundation and participating countries under  
536 management of the Joint Oceanographic Institutions (JOI), Inc. We thank Walter Hale and  
537 staff at the Bremen Core Repository for their help obtaining core material and also Mike  
538 Bolshaw, Dave Spanner, Richard Pearce, and Darryl Green for help with laboratory work.  
539 We also thank Paul Pearson, Mark Leckie and Bridget Wade for their helpful and  
540 constructive reviews of this work. Financial support was provided by the UK Natural  
541 Environment Research Council, award # NE/D005108/1.

542 **Footnotes**

543 <sup>1</sup> S. Crowhurst, Department of Earth Sciences, University of Cambridge, Downing  
544 Street, Cambridge, CB2 3EQ, United Kingdom, sjc13@cam.ac.uk



545 **References**

- 546 Anand, P., Elderfield, H. and Conte, M.H., 2003. Calibration of Mg/Ca thermometry in  
547 planktonic foraminifera from a sediment trap time series. *Paleoceanography*, 18(2):  
548 1050.
- 549 Barrera, E., Keller, G. and Savin, S.M., 1985. Evolution of the Miocene ocean in the eastern  
550 North Pacific as inferred from oxygen and carbon isotopic ratios of foraminifera. In:  
551 J.P. Kennett (Editor), *The Miocene Ocean: Palaeoceanography and Biogeography*.  
552 Geological Society of America Memoir 163, pp. 83-102.
- 553 Bemis, B.E., Spero, H.J., Bijma, J. and Lea, D.W., 1998. Reevaluation of the Oxygen  
554 Isotopic Composition of Planktonic Foraminifera: Experimental Results and Revised  
555 Paleotemperature Equations. *Paleoceanography*, 13(2): 150-160.
- 556 Bemis, B.E., Spero, H.J., Lea, D.W. and Bijma, J., 2000. Temperature influence on the  
557 carbon isotopic composition of *Globigerina bulloides* and *Orbulina universa*  
558 (planktonic foraminifera). *Marine Micropaleontology*, 38(3-4): 213-228.
- 559 Berner, R.A., 1991. A model for atmospheric CO<sub>2</sub> over Phanerozoic time. *American Journal*  
560 *of Science*, 291: 339-376.
- 561 Bernsen, E. and Dijkstra, H.A., 2010. Robustness of the Atlantic-Pacific flow reversal in the  
562 early miocene. *Climate of the Past Discussions*, 6(6): 2483-2516.
- 563 Billups, K., Channell, J.E.T. and Zachos, J., 2002. Late Oligocene to early Miocene  
564 geochronology and paleoceanography from the subantarctic South Atlantic.  
565 *Paleoceanography*, 17(1): 1004.
- 566 Biolzi, M., 1983. Stable isotopic study of Oligocene-Miocene sediments from DSDP Site  
567 354, Equatorial Atlantic. *Marine Micropaleontology*, 8(2): 121-139.
- 568 Bolli, H.M. and Saunders, J.B., 1989. Oligocene to Holocene low latitude planktic  
569 foraminifera. In: H.M. Bolli, J.B. Saunders and K. Perch-Nielsen (Editors), *Plankton*  
570 *stratigraphy*. Cambridge University Press, pp. 155-262.
- 571 Bornemann, A. and Norris, R.D., 2007. Size-related stable isotope changes in Late  
572 Cretaceous planktic foraminifera: Implications for paleoecology and photosymbiosis.  
573 *Marine Micropaleontology*, 65(1-2): 32-42.
- 574 Boyle, E.A. and Keigwin, L.D., 1985. Comparison of Atlantic and Pacific paleochemical  
575 records for the last 215,000 years: changes in deep ocean circulation and chemical  
576 inventories. *Earth and Planetary Science Letters*, 76(1-2): 135-150.
- 577 Broecker, W. and Yu, J., 2011. What do we know about the evolution of Mg to Ca ratios in  
578 seawater? *Paleoceanography*, 26(3): PA3203.
- 579 Burton, K.W., Gannoun, A. and Parkinson, I.J., 2010. Climate driven glacial-interglacial  
580 variations in the osmium isotope composition of seawater recorded by planktic  
581 foraminifera. *Earth and Planetary Science Letters*, 295(1-2): 58-68.
- 582 Burton, K.W. and Vance, D., 2000. Glacial-interglacial variations in the neodymium isotope  
583 composition of seawater in the Bay of Bengal recorded by planktonic foraminifera.  
584 *Earth and Planetary Science Letters*, 176(3-4): 425-441.
- 585 Chaisson, W.P. and Leckie, M.R., 1993. High-resolution Neogene planktonic foraminiferal  
586 biostratigraphy of Site 806, Ontong Java Plateau (western equatorial Pacific). In:  
587 W.H. Berger, L.W. Kroenke, T.R. Janecek and W.V. Sliter (Editors), *Proceedings of*  
588 *the Ocean Drilling Program, Scientific Results*, pp. 130: 137-178.
- 589 Channell, J.E.T. et al., 2003. Eocene to Miocene magnetostratigraphy, biostratigraphy, and  
590 chemostratigraphy at ODP Site 1090 (sub-Antarctic South Atlantic). *Geological*  
591 *Society of America Bulletin*, 115(5): 607-623.
- 592 Coggon, R.M., Teagle, D.A.H., Smith-Duque, C.E., Alt, J.C. and Cooper, M.J., 2010.  
593 *Reconstructing Past Seawater Mg/Ca and Sr/Ca from Mid-Ocean Ridge Flank*  
594 *Calcium Carbonate Veins*. *Science*, 327(5969): 1114-1117.

- 595 Coxall, H.K., Pearson, P.N., Shackleton, N.J. and Hall, M.A., 2000. Hantkeninid depth  
596 adaptation: An evolving life strategy in a changing ocean. *Geology*, 28(1): 87-90.
- 597 Coxall, H.K., Wilson, P.A., Pearson, P.N. and Sexton, P.F., 2007. Iterative evolution of  
598 digitate planktonic foraminifera. *Paleobiology*, 33(4): 495-516.
- 599 D'Hondt, S., Zachos, J.C. and Schultz, G., 1994. Stable Isotopic Signals and Photosymbiosis  
600 in Late Paleocene Planktic Foraminifera. *Paleobiology*, 20(3): 391-406.
- 601 Dickson, J.A.D., 2002. Fossil Echinoderms As Monitor of the Mg/Ca Ratio of Phanerozoic  
602 Oceans. *Science*, 298(5596): 1222-1224.
- 603 Elderfield, H. and Ganssen, G., 2000. Past temperature and  $\delta^{18}\text{O}$  of surface ocean waters  
604 inferred from foraminiferal Mg/Ca ratios. *Nature*, 405(6785): 442-445.
- 605 Elderfield, H., Vautravers, M. and Cooper, M., 2002. The relationship between shell size and  
606 Mg/Ca, Sr/Ca,  $\delta^{18}\text{O}$ , and  $\delta^{13}\text{C}$  of species of planktonic foraminifera. *Geochemistry*  
607 *Geophysics Geosystems*, 3(8): 1052.
- 608 Emiliani, C., 1955. Pleistocene temperatures. *The Journal of Geology*, 63: 40.
- 609 Frank, M., 2002. Radiogenic isotopes: Tracers of past ocean circulation and erosional input.  
610 *Rev. Geophys.*, 40(1): 1-38.
- 611 Gasperi, J.T. and Kennett, J.P., 1993. Vertical thermal structure evolution of Miocene surface  
612 waters: Western equatorial Pacific DSDP Site 289. *Marine Micropaleontology*, 22(3):  
613 235-254.
- 614 Greaves, M. et al., 2008. Interlaboratory comparison study of calibration standards for  
615 foraminiferal Mg/Ca thermometry. *Geochemistry Geophysics Geosystems*, 9(8):  
616 Q08010.
- 617 Green, D.R.H., Cooper, M.J., German, C.R. and Wilson, P.A., 2003. Optimization of an  
618 inductively coupled plasma-optical emission spectrometry method for the rapid  
619 determination of high-precision Mg/Ca and Sr/Ca in foraminiferal calcite.  
620 *Geochemistry Geophysics Geosystems*, 4.
- 621 Hall, J.M. and Chan, L.H., 2004. Li/Ca in multiple species of benthic and planktonic  
622 foraminifera: thermocline, latitudinal, and glacial-interglacial variation. *Geochimica*  
623 *et Cosmochimica Acta*, 68(3): 529-545.
- 624 Hardie, L.A., 1996. Secular variation in seawater chemistry: An explanation for the coupled  
625 secular variation in the mineralogies of marine limestones and potash evaporites over  
626 the past 600 m.y. *Geology*, 24(3): 279-283.
- 627 Hathorne, E.C., 2004. The Trace Element and Lithium Isotope Composition of Planktonic  
628 Foraminifera, Open University.
- 629 Hathorne, E.C. and James, R.H., 2006. Temporal record of lithium in seawater: A tracer for  
630 silicate weathering? *Earth and Planetary Science Letters*, 246(3-4): 393-406.
- 631 Hedberg, H.D., 1937. Foraminifera of the middle Tertiary Carapita Formation of northeastern  
632 Venezuela. *Journal of Paleontology*, 11(8): 661-697.
- 633 Hodell, D.A. and Vayavananda, A., 1993. Middle Miocene paleoceanography of the western  
634 equatorial Pacific (DSDP site 289) and the evolution of *Globorotalia* (Fohsella).  
635 *Marine Micropaleontology*, 22(4): 279-310.
- 636 Huh, Y., Chan, L.H. and Edmond, J.M., 2001. Lithium isotopes as a probe of weathering  
637 processes: Orinoco River. *Earth and Planetary Science Letters*, 194(1-2): 189-199.
- 638 Jeandel, C., 1993. Concentration and isotopic composition of Nd in the South Atlantic Ocean.  
639 *Earth and Planetary Science Letters*, 117(3-4): 581-591.
- 640 Keller, G., 1985. Depth stratification of planktonic foraminifers in the Miocene ocean. In:  
641 J.P. Kennett (Editor), *The Miocene Ocean: Palaeoceanography and Biogeography*.  
642 *Geological Society of America Memoir* 163, pp. 177-196.
- 643 Kennett, J.P. and Srinivasan, M.S., 1983. Neogene Planktonic Foraminifera: A Phylogenetic  
644 Atlas. Hutchinson Ross.

- 645 Kisakürek, B., James, R.H. and Harris, N.B.W., 2005. Li and  $\delta^7\text{Li}$  in Himalayan rivers:  
646 Proxies for silicate weathering? *Earth and Planetary Science Letters*, 237(3-4): 387-  
647 401.
- 648 Kroopnick, P.M., 1985. The distribution of  $^{13}\text{C}$  of  $\Sigma\text{CO}_2$  in the world oceans. *Deep Sea*  
649 *Research Part A. Oceanographic Research Papers*, 32(1): 57-84.
- 650 Kucera, M., Claude, H.-M. and Anne De, V., 2007. Chapter Six Planktonic Foraminifera as  
651 Tracers of Past Oceanic Environments, *Developments in Marine Geology*. Elsevier,  
652 pp. 213-262.
- 653 Kump, L.R. et al., 1999. A weathering hypothesis for glaciation at high atmospheric  $p\text{CO}_2$   
654 during the Late Ordovician. *Palaeogeography, Palaeoclimatology, Palaeoecology*,  
655 152(1-2): 173-187.
- 656 Lear, C.H., Elderfield, H. and Wilson, P.A., 2000. Cenozoic Deep-Sea Temperatures and  
657 Global Ice Volumes from Mg/Ca in Benthic Foraminiferal Calcite. *Science*,  
658 287(5451): 4.
- 659 Lear, C.H., Rosenthal, Y., Coxall, H.K. and Wilson, P.A., 2004. Late Eocene to early  
660 Miocene ice sheet dynamics and the global carbon cycle. *Paleoceanography*,  
661 19(PA4015): 1-11.
- 662 Leckie, R.M., Farnham, C. and Schmidt, M.G., 1993. Oligocene planktonic foraminifer  
663 biostratigraphy of Hole 803D (Ontong Java Plateau) and Hole 628A (Little Bahama  
664 Bank), and comparison with the southern high latitudes. In: W.H. Berger, L.W.  
665 Kroenke, T.R. Janecek and W.V. Sliter (Editors), *Proceedings of the Ocean Drilling*  
666 *Program, Scientific Results*, pp. 130: 113-136.
- 667 Levitus, S. and Boyer, T.P., 1994. *World Ocean Atlas 1994 Volume 4: Temperature*, 4.
- 668 Li, Q., McGowran, B. and Brunner C. A., 2002. Neogene Planktonic Foraminiferal  
669 Biostratigraphy of Sites 1126, 1128, 1130, 1132, and 1134, ODP Leg 182, Great  
670 Australian Bight. In: A.C. Hine, D.A. Feary and Malone M. J. (Editors), *Proceedings*  
671 *of the Ocean Drilling Program, Scientific Results*.
- 672 Liebrand, D. et al., 2011. Antarctic ice sheet and oceanographic response to eccentricity  
673 forcing during the early Miocene. *Climate of the Past*, 7(3): 869-880.
- 674 Miller, K.G., Wright, J.D. and Fairbanks, R.G., 1991. Unlocking the Ice House: Oligocene-  
675 Miocene Oxygen Isotopes, Eustasy, and Margin Erosion. *Journal of Geophysical*  
676 *Research*, 96(B4): 6829-6848.
- 677 Nathan, S.A. and Leckie, R.M., 2009. Early history of the Western Pacific Warm Pool during  
678 the middle to late Miocene (~ 13.2-5.8 Ma): Role of sea-level change and  
679 implications for equatorial circulation. *Palaeogeography, Palaeoclimatology,*  
680 *Palaeoecology*, 274(3-4): 140-159.
- 681 Norris, R.D., 1998. Recognition and macroevolutionary significance of photosymbiosis in  
682 molluscs, corals, and foraminifera. In: W.L. Manger and L.K. Meeks (Editors),  
683 *Isotope Paleobiology and Paleoecology. Paleontological Society Papers*, 4, pp. 68-  
684 100.
- 685 Norris, R.D., Corfield, R.M. and Cartlidge, J.E., 1993. Evolution of depth ecology in the  
686 planktic foraminifera lineage *Globorotalia* (Fohsella). *Geology*, 21(11): 975-978.
- 687 Norris, R.D. and Wilson, P.A., 1998. Low-latitude sea-surface temperatures for the mid-  
688 Cretaceous and the evolution of planktic foraminifera. *Geology*, 26(9): 823-826.
- 689 Olsson, R.K., Hemleben, C. and Pearson, P.N., 2006. Taxonomy, biostratigraphy and  
690 phylogeny of Eocene *Dentoglobigerina*. In: P.N. Pearson, R.K. Olsson, B.T. Huber,  
691 C. Hemleben and W.A. Berggren (Editors), *Atlas of Eocene Planktonic Foraminifera*.  
692 *Cushman Foundation Special Publication*, 41, pp. 401-412.
- 693 Pälike, H., Frazier, J. and Zachos, J.C., 2006a. Extended orbitally forced palaeoclimatic  
694 records from the equatorial Atlantic Ceara Rise. *Quaternary Science Reviews*, 25(23-  
695 24): 3138-3149.

- 696 Pälike, H. et al., 2006b. The Heartbeat of the Oligocene Climate System. *Science*, 314(5807):  
697 1894-1898.
- 698 Paul, H.A., Zachos, J.C., Flower, B.P. and Tripathi, A., 2000. Orbitally induced climate and  
699 geochemical variability across the Oligocene/Miocene boundary. *Paleoceanography*,  
700 15(5): 471.
- 701 Pearson, P.N. and Chaisson, W.P., 1997. Late Paleocene to middle Miocene planktonic  
702 foraminifer biostratigraphy of the Ceara Rise. In: N.J. Shackleton, W.B. Curry, C.  
703 Richter and T.J. Bralower (Editors), *Proceedings of the Ocean Drilling Program*,  
704 *Scientific Results*, pp. 154: 33-68.
- 705 Pearson, P.N., Norris, R.D. and Empson, A.J., 2001. *Mutabella mirabilis* Gen et Sp. Nov., a  
706 Miocene microperforate planktonic foraminifer with an extreme level of intraspecific  
707 variability. *Journal of Foraminiferal Research*, 31(2): 120-132.
- 708 Pearson, P.N. and Shackleton, N.J., 1995. Neogene Multispecies Planktonic Foraminifer  
709 Stable Isotope Record, Site 871, Limalok Guyot. In: J.A. Haggerty, I. Premoli Silva,  
710 F. Rack and M.K. McNutt (Editors), *Proceedings of the Ocean Drilling Program*,  
711 *Scientific Results*, pp. 144: 401-410.
- 712 Pearson, P.N., Shackleton, N.J. and Hall, M.A., 1993. Stable isotope paleoecology of middle  
713 Eocene planktonic foraminifera and multi-species isotope stratigraphy, DSDP Site  
714 523, South Atlantic. *Journal of Foraminiferal Research*, 23(2): 123-140.
- 715 Pearson, P.N., Shackleton, N.J., Weedon, G.P. and Hall, M.A., 1997. Multispecies planktonic  
716 foraminifera stable isotope stratigraphy through Oligocene/Miocene boundary  
717 climatic cycles, Site 926. In: N.J. Shackleton, Curry, W.B., Richter, C., and Bralower,  
718 T.J. (Editor), *Proceedings of the Ocean Drilling Program*, *Scientific Results*, pp. 154:  
719 441-449.
- 720 Pearson, P.N. and Wade, B.S., 2009. Taxonomy and stable isotope paleoecology of well-  
721 preserved planktonic foraminifera from the uppermost Oligocene of Trinidad. *Journal*  
722 *of Foraminiferal Research*, 39(3): 191-217.
- 723 Poore, R.Z. and Matthews, R.K., 1984. Oxygen isotope ranking of late Eocene and Oligocene  
724 planktonic foraminifera: Implications for Oligocene sea-surface temperatures and  
725 global ice-volume. *Marine Micropaleontology*, 9(2): 111-134.
- 726 Rathburn, A.E. and Corliss, B.H., 1994. The Ecology of Living (Stained) Deep-Sea Benthic  
727 Foraminifera from the Sulu Sea. *Paleoceanography*, 9(1): 87-150.
- 728 Ravelo, A.C. and Fairbanks, R.G., 1995. Carbon isotopic fractionation in multiple species of  
729 planktonic foraminifera from core-tops in the tropical Atlantic. *Journal of*  
730 *Foraminiferal Research*, 25(1): 53-74.
- 731 Ravizza, G. and Peucker-Ehrenbrink, B., 2003. The marine  $^{187}\text{Os}/^{188}\text{Os}$  record of the Eocene-  
732 Oligocene transition: the interplay of weathering and glaciation. *Earth and Planetary*  
733 *Science Letters*, 210(1-2): 151-165.
- 734 Raymo, M.E. and Ruddiman, W.F., 1992. Tectonic forcing of late Cenozoic climate. *Nature*,  
735 359(6391): 117-122.
- 736 Rosenthal, Y., Boyle, E.A. and Labeyrie, L., 1997. Last Glacial Maximum Paleochemistry  
737 and Deepwater Circulation in the Southern Ocean: Evidence From Foraminiferal  
738 Cadmium. *Paleoceanography*, 12(6): 787-796.
- 739 Rosenthal, Y., Field, M.P. and Sherrell, R.M., 1999. Precise determination of  
740 element/calcium ratios in calcareous samples using sector field inductively coupled  
741 plasma mass spectrometry. *Analytical Chemistry*, 71(15): 3248-3253.
- 742 Sexton, P.F., Wilson, P.A. and Pearson, P.N., 2006. Microstructural and geochemical  
743 perspectives on planktic foraminiferal preservation: "Glassy" versus "Frosty".  
744 *Geochemistry Geophysics Geosystems*, 7(12): Q12P19.
- 745 Shipboard Scientific Party, 1995a. Site 925. In: W.B. Curry, N.J. Shackleton, C. Richter and  
746 et al. (Editors), *Proceedings of the Ocean Drilling Program*. Initial Reports. College  
747 Station, TX (Ocean Drilling Program), pp. 154: 55-152.

- 748 Shipboard Scientific Party, 1995b. Site 926. In: W.B. Curry, N.J. Shackleton, C. Richter and  
749 et al. (Editors), Proceedings of the Ocean Drilling Program. Initial Reports. College  
750 Station, TX (Ocean Drilling Program), pp. 154: 153-232.
- 751 Smart, C.W. and Thomas, E., 2006. The enigma of early Miocene biserial planktic  
752 foraminifera. *Geology*, 34(12): 1041-1044.
- 753 Spero, H.J. and Williams, D.F., 1988. Extracting environmental information from planktonic  
754 foraminiferal  $\delta^{13}\text{C}$  data. *Nature*, 335(6192): 717-719.
- 755 Spero, H.J. and Williams, D.F., 1989. Opening the Carbon Isotope "Vital Effect" Black Box  
756 1. Seasonal Temperatures in the Euphotic Zone. *Paleoceanography*, 4(6): 593-601.
- 757 Spezzaferri, S., 1994. Planktonic foraminiferal biostratigraphy and taxonomy of the  
758 Oligocene and lower Miocene in the oceanic record. An overview. *Palaeontographia*  
759 *Italica*, 81: 188.
- 760 Spezzaferri, S. and Pearson, P.N., 2009. Distribution and Ecology of *Catapsydrax indianus*,  
761 A New Planktonic Foraminifer Index Species for the Late Oligocene–Early Miocene.  
762 *Journal of Foraminiferal Research*, 39(2): 112-119.
- 763 Stainforth, R.M., Lamb, J.L., Luterbacher, H., Beard, J.H. and Jeffords, R.M., 1975.  
764 Cenozoic Planktonic Foraminiferal Zonation and Characteristics of Index Forms  
765 (Appendix), Article 62. *Univ. Kansas Paleontol. Contrib.*
- 766 Stanley, S.M. and Hardie, L.A., 1998. Secular oscillations in the carbonate mineralogy of  
767 reef-building and sediment-producing organisms driven by tectonically forced shifts  
768 in seawater chemistry. *Palaeogeography, Palaeoclimatology, Palaeoecology*, 144(1-  
769 2): 3-19.
- 770 Tyrrell, T. and Zeebe, R.E., 2004. History of carbonate ion concentration over the last 100  
771 million years. *Geochimica et Cosmochimica Acta*, 68(17): 3521-3530.
- 772 Vance, D. and Burton, K., 1999. Neodymium isotopes in planktonic foraminifera: a record of  
773 the response of continental weathering and ocean circulation rates to climate change.  
774 *Earth and Planetary Science Letters*, 173(4): 365-379.
- 775 Vance, D., Teagle, D.A.H. and Foster, G.L., 2009. Variable Quaternary chemical weathering  
776 fluxes and imbalances in marine geochemical budgets. *Nature*, 458(7237): 493-496.
- 777 von der Heydt, A. and Dijkstra, H.A., 2005. Flow reorganizations in the Panama Seaway: A  
778 cause for the demise of Miocene corals? *Geophys. Res. Lett.*, 32(2): L02609.
- 779 von der Heydt, A. and Dijkstra, H.A., 2006. Effect of ocean gateways on the global ocean  
780 circulation in the late Oligocene and early Miocene. *Paleoceanography*, 21(1):  
781 PA1011.
- 782 Wade, B., Al-Sabouni, N., Hemleben, C. and Kroon, D., 2008. Symbiont bleaching in fossil  
783 planktonic foraminifera. *Evolutionary Ecology*, 22(2): 253-265.
- 784 Wade, B.S., Berggren, W.A. and Olsson, R.K., 2007. The biostratigraphy and paleobiology  
785 of Oligocene planktonic foraminifera from the equatorial Pacific Ocean (ODP Site  
786 1218). *Marine Micropaleontology*, 62(3): 167-179.
- 787 Wade, B.S. and Pälike, H., 2004. Oligocene climate dynamics. *Paleoceanography*, 19(4):  
788 PA4019.
- 789 Walker, J.C.G., Hays, P.B. and Kasting, J.F., 1981. A negative feedback mechanism for the  
790 long-term stabilization of the Earth's surface temperature. *Journal of Geophysical*  
791 *Research*, 86(C10): 9776-9782.
- 792 Weedon, G.P., Shackleton, N.J. and Pearson, P.N., 1997. The Oligocene time scale and  
793 cyclostratigraphy on the Ceara Rise, western equatorial Atlantic. In: N.J. Shackleton,  
794 Curry, W.B., Richter, C., and Bralower, T.J. (Editor), Proceedings of the Ocean  
795 Drilling Program, Scientific Results, pp. 154: 101-114.
- 796 Wilkinson, B.H. and Algeo, T.J., 1989. Sedimentary carbonate record of calcium-magnesium  
797 cycling. *American Journal of Science*, 289(10): 1158-1194.

798 Zachos, J.C., Shackleton, N.J., Revenaugh, J.S., Palike, H. and Flower, B.P., 2001. Climate  
799 response to orbital forcing across the Oligocene-Miocene boundary. *Science*,  
800 292(5515): 274-278.  
801  
802  
803